

## Effects of Degree of Mixing on Quantitative Interpretation of TPD Spectra

THEOPHILOS IOANNIDES AND XENOPHON E. VERYKIOS

*Institute of Chemical Engineering and High Temperature Chemical Processes, Department of Chemical Engineering, University of Patras, Patras, Greece*

Received August 11, 1988; revised June 8, 1989

The influence of the degree of mixing on the qualitative and quantitative interpretation of TPD spectra is investigated by simulation of physicochemical processes occurring within TPD cells. A methodology for accounting for readsorption effects is also developed and utilized in the simulations. It is shown that, as a result of imperfect mixing conditions, peak temperatures shift to lower values. Computed values of the heat of adsorption and the preexponential factor of desorption are always less than the true values, which can be obtained only under conditions of perfect mixing. Errors introduced by the presence of axial concentration gradients are large when desorption follows first-order kinetics and significantly smaller when second-order desorption kinetics are followed. An experimental procedure accounting for mixing effects is proposed. © 1989 Academic Press, Inc.

### INTRODUCTION

Temperature-programmed desorption (TPD) is a widely used technique of characterization and study of catalysts, which has mainly been applied to supported metals. The method can give valuable information concerning the interaction of an adsorbent with an adsorbate, mainly pertaining to the state of the adsorbate, bond strengths, and surface chemical transformations. Because of the uncertainties involved in TPD experiments, in most cases TPD spectra are analyzed only qualitatively. Nevertheless, methods for quantitative analysis of TPD spectra do exist (1-6). These methods are based on the assumption that intraparticle and interparticle mass diffusional resistances are negligible and that perfect mixing within the catalyst bed exists, which can then be modeled as a continuous stirred tank reactor (CSTR). In recent years, a number of theoretical studies have explored these assumptions and have investigated the influence of several parameters on the phenomena which take place during a TPD experiment.

Herz *et al.* (7) examined readsorption effects during TPD of CO from supported Pt catalysts and concluded that readsorption is almost impossible to eliminate. Thus, it should always be taken into account in the quantitative analysis of TPD spectra. Similarly, Rieck and Bell (5) demonstrated that the shape and position of TPD spectra are affected by readsorption and intraparticle mass transfer resistances. The relative importance of these phenomena depends on specific values of experimental parameters such as catalyst particle size and carrier gas flow rate. Analysis of TPD spectra which have been influenced by mass transport resistances can lead to significant errors in the estimation of kinetic or thermodynamic parameters.

Demmin and Gorte (8, 9) have presented a group of dimensionless numbers which define the relative importance of phenomena such as intraparticle mass transport, readsorption, and axial dispersion, during a TPD experiment. These numbers are defined by experimental parameters and thus can function as a useful guide in the design of proper TPD experiments. The validity of

the criterion on intraparticle mass transport was also confirmed by the work of Huang *et al.* (10). Other investigators have also studied mass transport effects, either theoretically (11) or experimentally (12).

The requirement of perfect mixing in a TPD cell has been well established and a criterion for the absence of axial gradients has been stated (9). Nevertheless, no analysis of the influence of different mixing conditions on the resulting TPD spectra exists in the literature. For practical purposes, such an analysis is very useful since attainment of perfect mixing conditions in a TPD experiment, in many cases, is very difficult. To attain perfect mixing, the catalyst bed must be very short and the carrier gas flow rate significantly low, conditions which can create problems in detection of the desorbing species and increased mass transport resistances. The purpose of this theoretical analysis is to qualitatively elucidate changes in shape and position of TPD spectra due to axial concentration gradients along a TPD cell, and to analyze possible errors which might arise in the quantitative interpretation of TPD spectra obtained under conditions of imperfect mixing of various degrees. In the present analysis intraparticle and interparticle mass diffusional resistances have been assumed to be negligible.

#### NOTATION

$A$	Ratio of preexponential factors for desorption and adsorption ( $\text{mol cm}^{-3}$ )
$A_a$	Preexponential factor of adsorption ( $\text{cm}^3 \text{mol}^{-1} \text{s}^{-1}$ )
$A_d$	Preexponential factor of desorption ( $\text{s}^{-1}$ )
$C$	Gas-phase concentration ( $\text{mol cm}^{-3}$ )
$D_e$	Effective diffusivity in the TPD bed ( $\text{cm}^2 \text{s}^{-1}$ )
$D_T$	Tube diameter (cm)
$d_p$	Particle diameter (cm)
$E_a$	Activation energy of adsorption ( $\text{kcal mol}^{-1}$ )

$E_d$	Activation energy of desorption ( $\text{kcal mol}^{-1}$ )
$\Delta H$	Heat of adsorption ( $\text{kcal mol}^{-1}$ )
$L$	Length of catalyst bed (cm)
$N$	Number of CSTRs used to simulate the TPD bed
$n$	Order of desorption or adsorption
$Pe_L$	Axial Peclet number
$Pe_d$	Peclet number based on particle diameter
$Q$	Volumetric flow rate of carrier gas ( $\text{cm}^3 \text{s}^{-1}$ )
$S$	Sticking coefficient
$S_0$	Initial sticking coefficient
$T$	Temperature (K)
$t$	Time (s)
$u$	Superficial velocity of the carrier gas ( $\text{cm s}^{-1}$ )
$\bar{u}$	Interstitial velocity of the carrier gas ( $\text{cm s}^{-1}$ )
$V$	Initial amount of adsorbate (at $\theta_0 = 1$ ) per unit volume of bed ( $\text{mol cm}^{-3}$ )
$V_t$	Initial amount of adsorbate in bed, at $\theta_0 = 1$ (mol)
$\beta$	Heating rate (K/s)
$\epsilon_B$	Bed void fraction
$\zeta$	Dimensionless bed length
$\theta$	Surface coverage
$\sigma$	Surface area per mole of exposed metal atom ( $\text{cm}^2 \text{mol}^{-1}$ )

#### THEORETICAL ANALYSIS

##### *Perfect Mixing Case*

Under conditions of perfect mixing, gas phase concentration and surface coverage are uniform throughout the TPD bed. The mass conservation equation in this case can be written in the form

$$C = -\frac{VL}{u} \beta \frac{d\theta}{dT}. \quad (1)$$

The parameter which is measured in a TPD experiment is the concentration of the adsorbate in the carrier gas at the exit of the catalyst bed. This exit concentration depends on the rate of desorption,  $d\theta/dT$ . If the TPD bed operates under conditions of

perfect mixing, or as a CSTR, the concentration of the adsorbate within the bed,  $C$ , is by definition equal to the measured exit concentration. Methods for quantitative analysis of TPD spectra so as to obtain thermodynamic and kinetic parameters of adsorption under these conditions are available (1-6).

The gas phase concentration,  $C$ , is related to the surface coverage via the equation (2, 5, 7, 13)

$$C = \frac{(VL/u)k_d\theta^n}{1 + (VL/u)FS}. \quad (2)$$

The superficial velocity,  $u$ , is proportional to temperature:

$$u = u_0 \frac{T}{T_0}. \quad (3)$$

Equation (2) can be made dimensionless by introducing the dimensionless variables

$$C_r = \frac{C}{C_m}, \quad T_r = \frac{T}{T_m} \quad (4)$$

where  $C_m$  is the maximum observable concentration of the adsorbate in the carrier gas in the case in which readsorption is insignificantly small, and  $T_m$  is the temperature at which maximum concentration is observed.

If readsorption of desorbed gas is a dominant factor, as in many practical cases (4, 7, 9),  $(VL/u)FS \gg 1$  and Eq. (2) reduces to

$$C_r = \frac{K_d\theta^n}{C_mFS}. \quad (5)$$

For given desorption kinetics and heating rate,  $T_m$  is independent of any other parameter, while  $C_m$  depends additionally on the ratio  $(VL/u_0)$  (or, equivalently, on  $V_t/Q_0$ ) (1). Then, Eq. (5) implies that  $C_r$  is proportional to  $Q_0/V_t \cdot S_0$  which means that, for given desorption kinetics and heating rate, the value of the ratio  $Q_0/V_t \cdot S_0$  defines a certain dimensionless TPD curve, irrespectively of the individual values of the parameters  $Q_0$ ,  $V_t$ , and  $S_0$ . Readsorption effects are also governed by the same term. As ex-

pected, readsorption is favored by high values of  $V_t$  and  $S_0$  and low values of  $Q_0$ . Therefore, the influence of readsorption on the observed TPD curves can be investigated by examining the influence of one parameter only, namely,  $Q_0/V_t S_0$ . This conclusion is valid under any mixing conditions within the TPD cell since a series of perfect mixers can be employed to describe the entire process. Its validity has been examined over a large range of parameter values and mixing conditions.

#### Plug Flow Case

When the flow pattern in a TPD cell is such that no axial mixing of the carrier gas occurs, the concentration of the adsorbate can vary along the bed length, and the mass balance equation which describes the adsorbate concentration as a function of position and temperature is

$$\frac{\partial C}{\partial \zeta} = -\frac{VL}{u} \beta \frac{\partial \theta}{\partial T} \quad (6)$$

with initial and boundary conditions:

$$\begin{aligned} \text{at } T = T_0 (t = 0), \quad C(\zeta) = 0, \quad \theta(\zeta) = \theta_0 \\ \text{at } \zeta = 0, \quad C = 0 \\ \text{at } \zeta = 1, \quad \partial C / \partial \zeta = 0. \end{aligned}$$

Gas phase concentration and surface coverage, in this case, are not uniform throughout the bed. Thus, the rate of desorption varies along the bed length and the measured concentration is only an indication of an average desorption rate.

These considerations are valid only in the case in which readsorption of the desorbed gas is important. If readsorption does not occur the gas phase concentration does not influence desorption kinetics and the computed TPD curves are identical, irrespectively of mixing conditions within the catalyst bed.

#### Intermediate Mixing Case

The cases discussed earlier represent two limits in the operation of a TPD cell, namely, perfect mixing and complete absence of mixing. In reality, under a broad

range of operating conditions, an intermediate degree of mixing exists within the cell. A TPD bed with an intermediate degree of mixing can be viewed either as a series of cells each of which operates under conditions of complete mixing, or as a single cell in which axial dispersion produces back-mixing of the adsorbate gas.

In the perfectly mixed series of cells configuration, the material balance yields

$$C_i = C_{i-1} - \frac{VL}{uN} \beta \frac{d\theta}{dT}, \quad i = 1, 2, \dots, N \quad (7)$$

where  $i$  is the cell index and  $N$  the total number of cells.

If the axial dispersion model is used, the material balance yields

$$\frac{1}{Pe_L} \frac{\partial^2 C}{\partial \zeta^2} - \frac{\partial C}{\partial \zeta} = \frac{VL}{u} \beta \frac{\partial \theta}{\partial T} \quad (8)$$

with boundary conditions

$$\begin{aligned} \text{at } \zeta = 0, \quad C &= \frac{1}{Pe_L} \left. \frac{\partial C}{\partial \zeta} \right|_{\zeta=0} \\ \text{at } \zeta = 1, \quad \left. \frac{\partial C}{\partial \zeta} \right|_{\zeta=1} &= 0 \end{aligned}$$

The axial Peclet number,  $Pe_L$ , defines the degree of mixing in the TPD bed. As  $Pe_L$  approaches infinity, conditions of plug flow (no mixing) in the bed are approached and Eq. (8) reduces to Eq. (6). As  $Pe_L$  approaches zero, conditions of perfect mixing in the bed are approached.

The axial Peclet number based on bed length,  $Pe_L$ , defined as  $Pe_L = uL/D_e$ , can be estimated through the Peclet number based on catalyst particle diameter, defined by  $Pe_d = d_p u/D_e$ .  $Pe_d$  can be estimated through empirical correlations and it is expressed as a function of Reynolds and Schmidt numbers in the form (14)

$$\frac{1}{Pe_d} = \frac{0.3}{Re Sc} + \frac{0.5}{1 + 3.8(Re Sc)^{-1}} \quad (9)$$

$Pe_L$  is then related to  $Pe_d$  by

$$Pe_L = \frac{\varepsilon_\beta L}{d_p} Pe_d. \quad (10)$$

A parameter which cannot be estimated with a high degree of confidence, unless measured experimentally, is the effective diffusivity,  $D_e$ , of the adsorbate gas within the catalyst bed. Thus, the Peclet number cannot always be known very accurately. It must also be noted that the Peclet number is a function of temperature, being inversely proportional to the square root of temperature. Thus,  $Pe_L$  decreases during a TPD run (15). To be able to compare results, all Peclet numbers are estimated at a reference temperature of 300 K, while the same heating rate was assumed in all cases.

The axial dispersion model is more realistic than the perfectly mixed series of cells as a model for the simulation of a TPD experiment because it does take into account the increase in the degree of mixing with increasing temperature during an experimental run. Because of this difference between the two models, equivalence between them is not straightforward.

To investigate theoretically the effects of mixing conditions on the shape and position of a TPD curve, all other factors which influence these parameters must be kept constant. For a given system, the degree of mixing depends on bed length and carrier gas velocity. These two parameters also affect the degree of readsorption. Thus, in an attempt to study the effects of degree of mixing alone, these two parameters must be varied in such a way that the same extent of readsorption is assumed. This can be accomplished if  $L$  and  $u$  are varied in such a way that their ratio  $L/u$  remains constant. Then the term  $VL/u_0$ , or, equivalently,  $V_i/Q_0$ , will remain constant and, for reasons stated earlier, the extent of readsorption will also remain constant.

#### Quantitative Analysis of TPD Spectra

Under the assumptions of perfect mixing within the TPD cell, free readsorption of

the desorbed gas, and heat of adsorption independent of surface coverage, it can be inferred that (3)

$$\ln \left[ \frac{T_m^2 \theta_m^{n-1}}{(1 - \theta_m)^{n+1} \beta} \right] = \frac{\Delta H}{RT_m} + \ln \left[ \frac{VL(\Delta H)}{unAR} \right] \quad (11)$$

where  $\Delta H$  is the heat of adsorption and  $A$  is the ratio of preexponential factors for desorption and adsorption,  $A = A_d/A_a$ .  $\Delta H$  and  $A$  can be determined by application of the linear relationship of Eq. (2) from the slope and the intercept. Experimentally, values of  $T_m$  and  $\theta_m$  can be obtained by varying the initial surface coverage,  $\theta_0$ , or, alternatively, the heating rate,  $\beta$ .

Equation (11) has been developed under the assumption that the preexponential factors  $A_a$  and  $A_d$  are independent of temperature. Nevertheless, the adsorption preexponential factor is a weak function of temperature, of the form

$$A_a = A_a^0 T^{1/2}. \quad (12)$$

If this fact is taken into account, Eq. (11) assumes the more complicated form

$$\ln \left[ \frac{T_m^{2.5} \theta_m^{n-1}}{(2\Delta H - RT_m)(1 - \theta_m)^{n+1} \beta} \right] = \frac{\Delta H}{RT_m} + \ln \left[ \frac{VLT_0}{2nu_0RA^*} \right] \quad (13)$$

where  $A^* = A_d/A_a^0$ . Using Eq. (13),  $\Delta H$  and  $A^*$  can be determined by a trial and error procedure. In the course of this work, it was found that convergence is fast if a reasonable value of  $\Delta H$  is assumed initially. It was also found necessary to employ Eq. (13) in the quantitative analysis of TPD spectra since the error introduced by employment of Eq. (11) is not negligible.

As stated earlier, Eqs. (11) and (13) have been developed under the assumption of perfect mixing within the catalyst bed. Deviations which originate from the presence of concentration gradients within the bed were investigated and results are presented in the following section.

## RESULTS AND DISCUSSION

The mathematical models described in the previous section were employed to simulate TPD spectra under different mixing conditions. To make the simulation more realistic, parameter values pertaining to the desorption of hydrogen from a group VIII metal surface were employed. Values of rate parameters for the desorption process were chosen to be representative of values existing in the literature, while the adsorption rate parameter  $S_0$  was varied over a wide range so that readsorption effects could be studied. The ranges of parameter values, along with chosen values of experimental parameters, are listed in Table 1. Experimental parameters are representative of those used in TPD experiments.

The continuous stirred tank reactor (CSTR) and plug flow reactor (PFR) models describe two limiting cases in the degree of mixing within a TPD cell, namely complete or perfect mixing and absence of mixing, respectively. Thus, these two models define the space of mixing effects which might be expected in a TPD experiment. TPD spectra described by the CSTR and PFR models, for first- and second-order desorption kinetics, are shown in Figs. 1 and 2, respectively. The curves, which are presented in the dimensionless form as described earlier, were computed on the assumption that the catalyst bed contains

TABLE 1

Parameter Values Used to Simulate TPD Spectra	
$A_d$	$10^{13} \text{ s}^{-1}$
$E_d$	25 kcal/mol
$S_0$	$10^{-6}$ – $10^0$
$E_a$	0 kcal/mol
$\beta$	1 k/s
$d_p$	0.025 cm
$D_T$	1.0 cm
$Q_{300 \text{ K}}$	1.5–6 cm <sup>3</sup> /s
$m$	0.09–0.3 g
$\epsilon_B$	0.5
$\sigma$	$4.0 \times 10^8 \text{ cm}^2/\text{mol}$

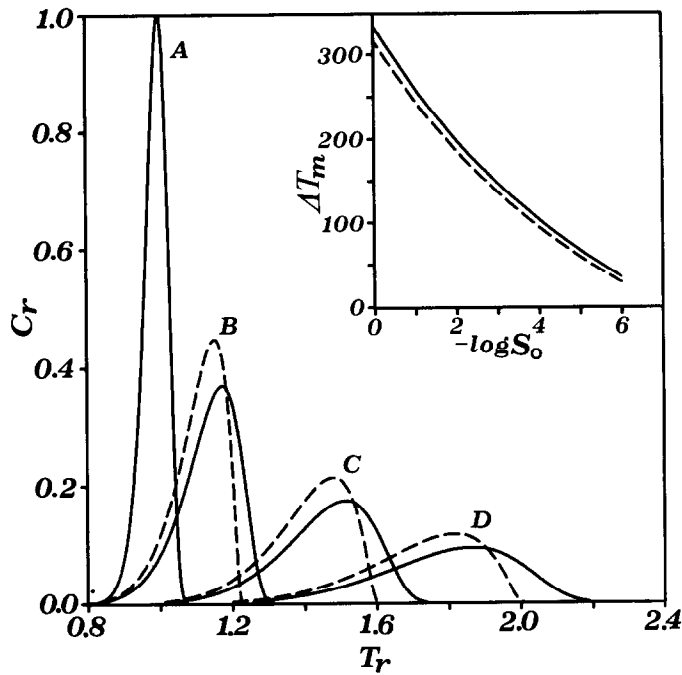


FIG. 1. Simulated first-order TPD spectra under PFR (---) and CSTR (—) conditions.  $S_0$ : A = 0; B =  $10^{-5}$ ; C =  $10^{-2}$ ; D =  $10^0$ . Inset: Peak temperature shift as a function of  $S_0$ .

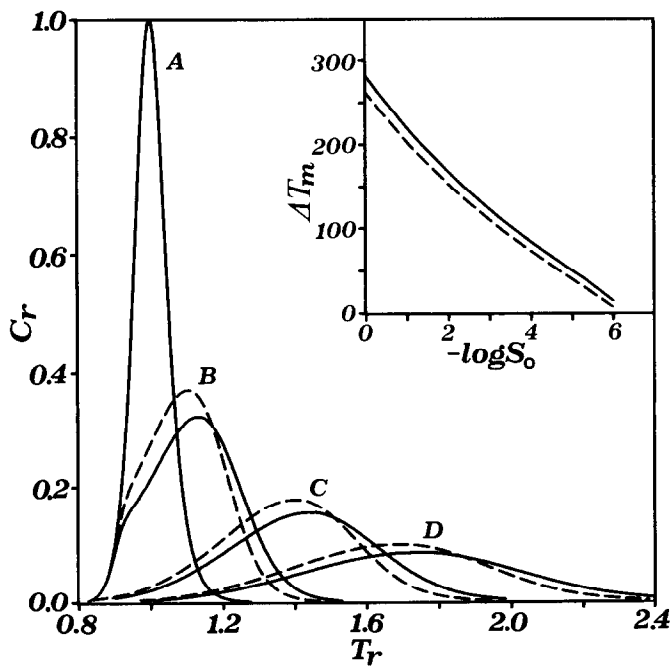


FIG. 2. Simulated second-order TPD spectra (symbols identical to those in Fig. 1).

0.118 g of catalyst and the carrier gas flow rate is  $2.0 \text{ cm}^3/\text{s}$ . In a TPD experiment, the degree of readsorption can be characterized and quantified by the initial sticking coefficient,  $S_0$ . The importance of readsorption increases with increasing value of the sticking coefficient. When  $S_0$  assumes the value of zero, no readsorption occurs. In that case, as stated earlier, TPD spectra are identical, irrespective of mixing conditions. This is illustrated in Figs. 1 and 2 by curve A which is identical in both the CSTR and PFR models. An examination of Figs. 1 and 2 indicates that readsorption of the desorbed gas exerts three major effects on the position and shape of TPD spectra: (1) Peaks shift to higher temperatures as the degree of readsorption ( $S_0$ ) increases. This observation is valid for both first- and second-order kinetics and for CSTR and PFR mixing conditions. While the temperature shift is approximately 40–60 K when  $S_0$  has the value of  $10^{-5}$ , it can reach 300–350 K when  $S_0$  assumes the value of unity. The insets in Figs. 1 and 2 show the magnitude of peak temperature shifts as a function of the initial sticking coefficient. Temperature shifts are significant in all cases considered and they become negligible at values of  $S_0$  less than  $10^{-6}$ , which are unrealistically low. (2) As the degree of readsorption increases, the exit concentration of desorbed gas decreases. Thus, when  $S_0$  has the value of  $10^{-5}$ , the maximum concentration is about 50% of that observed in the absence of readsorption ( $S_0 = 0$ ), while, when  $S_0$  is 1, it is only 10%. (3) TPD peaks become broader with increasing value of  $S_0$ . In the absence of readsorption, desorption occurs in a rather narrow temperature range, which in the case presented is about 100 K. Under strong readsorption conditions the TPD curves extend over a range of about 400 K. In such cases it is difficult experimentally to identify peak temperatures with accuracy. Curves describing second-order desorption kinetics are, in general, broader but more symmetric than first-order desorption curves.

It should be noted that readsorption exerts a significant influence on the shape and position of TPD peaks even at a value of initial sticking coefficient as low as  $10^{-5}$ . A typical value of  $S_0$  for hydrogen adsorption on a group VIII metal surface is on the order of  $10^{-1}$ . To bring the readsorption effects to the level observed with  $S_0$  equal to  $10^{-5}$ , the ratio  $V_1/Q_0$  should be at least  $10^4$  times smaller. This would require the use of 1 mg of catalyst in the bed with a carrier gas flow rate of  $200 \text{ cm}^3/\text{s}$ . These experimental conditions are not easily achievable. Moreover, the exit concentration would be undetectably low under such conditions. This example clearly demonstrates that, in most cases, readsorption cannot be experimentally eliminated and its effect on TPD spectra must be accounted for, in agreement with results of other investigations (4, 7, 8, 9).

In the absence of any mixing within the TPD cell (PFR case), peaks appear at a lower temperature for both first- and second-order desorption kinetics and the maximum concentration is larger than that of the CSTR case. The second observation is due to the fact that PFR peaks are narrower than CSTR ones and considerably less symmetric. These differences are more pronounced in first-order desorption kinetics. The effects of mixing conditions on TPD spectra can be explained if the adsorption/desorption process is visualized as a reversible chemical reaction taking place in a stirred tank or plug flow reactor which, in this case, is the TPD bed. In that situation mixing has a negative influence on the performance of the reactor which, in the TPD case, is manifested as higher temperature desorption peaks and broader ones.

It is also observed in Fig. 2 (curve B) that a shoulder appears on the TPD curve. The presence and magnitude of this shoulder were found to depend on the value of  $S_0$  and the activation energy of adsorption. Obviously, the presence of this shoulder is due to inherent parameters of the process. It has already been shown (13) that for certain

combinations of kinetic and experimental parameters, rather distorted TPD spectra can be obtained. Thus, care must be exercised in interpreting the appearance of such shoulders in TPD curves, since these might not be due to surface inhomogeneities or adsorbate-adsorbent interactions of different kinds, as normally attributed.

As the degree of mixing in a TPD cell decreases, TPD curves are expected to move gradually from the CSTR position toward the PFR position. This is illustrated in Fig. 3 for first- and second-order desorption kinetics. Intermediate degrees of mixing are characterized by the Peclet number, which is zero under conditions of complete mixing and infinity in the absence of any mixing. It is apparent from Fig. 3 that the degree of mixing exerts a more significant influence on TPD curves under first-order kinetics.

The effects of degree of mixing on the qualitative and quantitative interpretation of TPD spectra have been investigated extensively employing the axial dispersion model presented in the previous section. TPD spectra were computed for three different values of the initial sticking coefficient,  $S_0$ , namely  $10^{-4}$ ,  $10^{-2}$ , and 1. The Peclet numbers used and the corresponding values of experimental parameters, which are within the range of values encountered in TPD experiments, are listed in Table 2. In all cases, the ratio  $VL/u_0$ , or, alternatively,  $V_t/Q_0$ , was maintained at the same value, ensuring the same degree of readorption and identical influence of this parameter in all cases. Thus, whatever changes are observed are only due to different mixing conditions.

Taking the CSTR as a reference case, differences in peak temperatures were com-

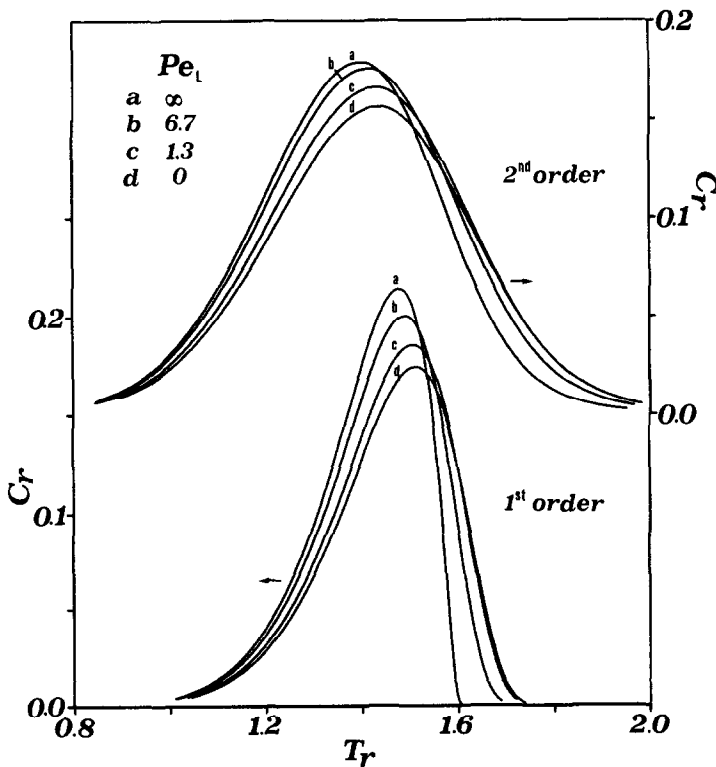


FIG. 3. Effects of degree of mixing on shape and position of TPD spectra under first- and second-order kinetics.



TABLE 2

 Parameter Values Assumed in the Investigation of  
 Mixing Effects on TPD Spectra

$Pe_L$	Bed length (cm)	Velocity of carrier gas (cm/s)	Catalyst weight (g)	Volumetric flow rate (cm <sup>3</sup> /s)
0.8	0.2	2.0	0.094	1.6
1.3	0.25	2.5	0.118	2.0
1.9	0.30	3.0	0.142	2.4
3.0	0.37	3.7	0.177	3.0
6.7	0.56	5.6	0.265	4.5
11.8	0.75	7.5	0.354	6.0

puted as a function of the Peclet number. Negative shifts in peak temperature as a function of Peclet number with  $S_0$  as a parameter are illustrated in Fig. 4 for first-order desorption kinetics. Similar results were also obtained for second-order kinetics. It is apparent that shifts increase with increasing value of the initial sticking coefficient,  $S_0$ . It should also be noted that for  $Pe_L$  values less than unity, differences in

peak temperatures are less than 3 K, for all cases considered.

To estimate kinetic and thermodynamic parameters, values of  $T_m$  and  $\theta_m$  are required. Such values were obtained by variation of initial surface coverage,  $\theta_0$ . In cases in which axial concentration gradients exist,  $\theta_m$  varies along the length of the catalyst bed. In that case, an average surface coverage,  $\bar{\theta}_m$ , was computed, at the temperature  $T_m$ , from the relationship

$$\bar{\theta}_m = \frac{\int \theta(\zeta) d\zeta}{\int d\zeta}. \quad (14)$$

Representative TPD spectra of first-order desorption kinetics, obtained under different initial surface coverages, are shown in Fig. 5 for Peclet values of zero and infinity. The spectra simulated under no mixing conditions ( $Pe_L = \infty$ ) do not have the usual symmetric appearance as the absence of mixing produces significant distortion in their shape.

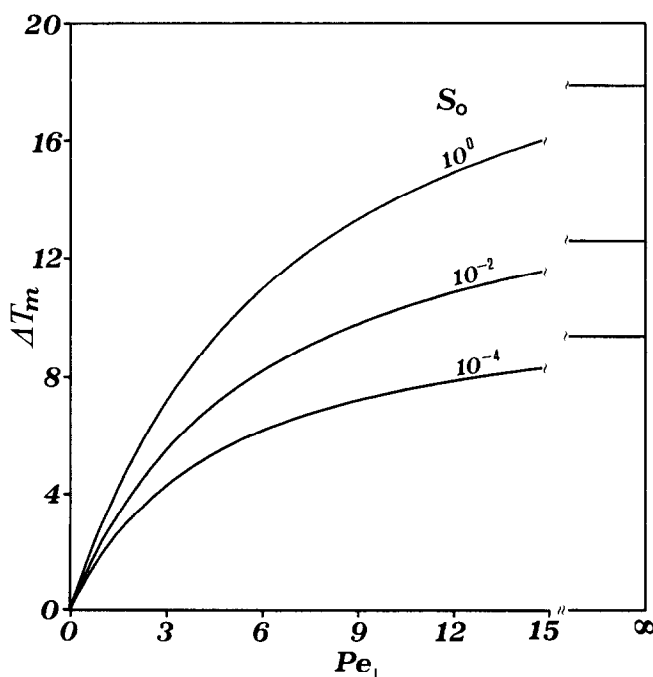


FIG. 4. Peak temperature shifts due to imperfect mixing of various degrees within TPD cells.

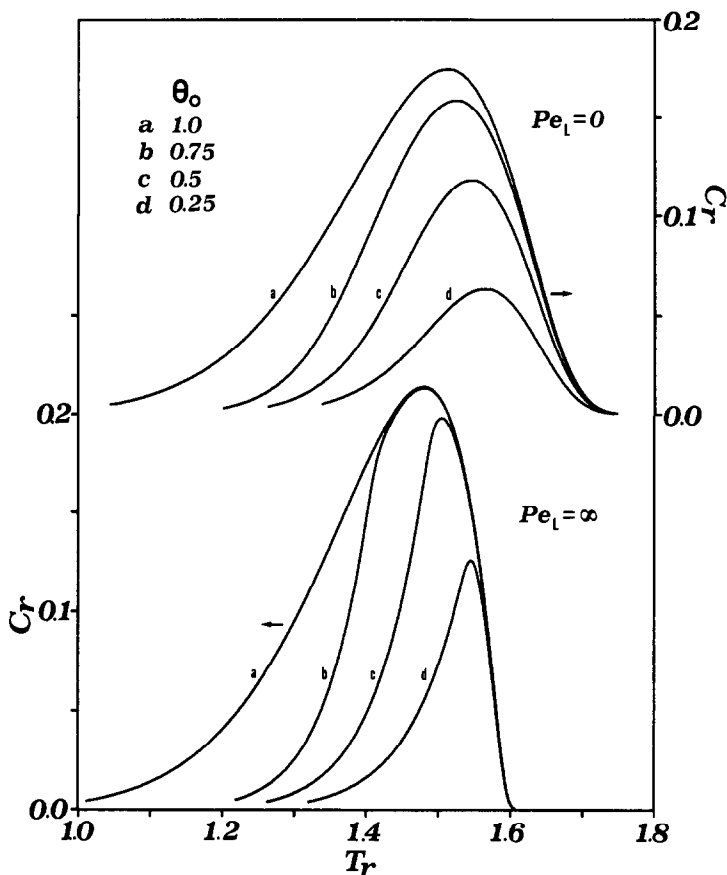


FIG. 5. First-order TPD spectra obtained for different initial surface coverages under CSTR and PFR conditions.

These spectra were analyzed, following Eq. (13), to determine the values of  $\Delta H$  and  $A_d$ . These values are then compared with the corresponding values which were used in the generation of the spectra. It should be noted at this point that if Eq. (11) is used to analyze the spectra, significant errors in the estimation of  $\Delta H$  and  $A_d$  are introduced. Thus, Eq. (13) must be employed in analyses of the type described in this section. The added difficulty in using Eq. (13) is more than adequately compensated by the accuracy of the results obtained.

The computed values for the CSTR case ( $Pe_L = 0$ ) were found to be identical to the corresponding values used in the simulation of the spectra, namely,  $\Delta H = -25.0$  kcal/mol and  $A_d = 1.0 \times 10^{13} \text{ s}^{-1}$ . This accuracy

is expected since Eq. (13) has been developed under the assumption of complete mixing within the TPD cell. As expected, under conditions of imperfect mixing, deviations between the true and computed values arise. Differences between the true and computed values of  $\Delta H$  are shown in Fig. 6 as a function of the Peclet number with  $S_0$  as a parameter, for first- and second-order kinetics. The estimated values of  $\Delta H$  are always less than the true value of  $-25$  kcal/mol and the difference increases with increasing Peclet number and decreases with increasing initial sticking coefficient,  $S_0$ , or degree of readsorption.

It should be noted that under first-order desorption kinetics, for  $Pe_L$  values less than unity, in all cases, the difference in  $\Delta H$  is

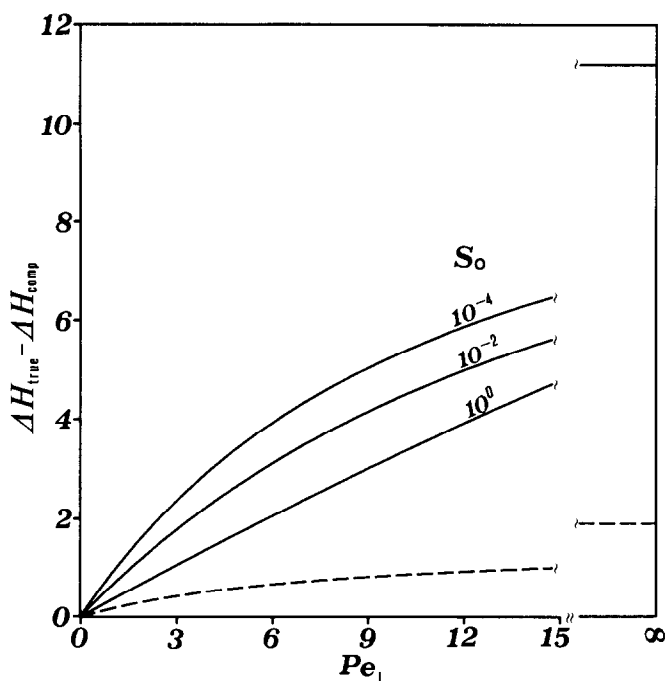


FIG. 6. Difference between true and computed heat of adsorption for first-order (—) and second-order (---) kinetics.

less than 1 kcal/mol or less than 4%. Under second-order desorption kinetics, although computed values of  $\Delta H$  are always less than the true values, the differences are only minor. Even when  $Pe_L$  approaches infinity (plug flow case), the estimated  $\Delta H$  differs from the true  $\Delta H$  by only 2 kcal/mol or by 8%. Thus, in cases in which desorption follows second-order kinetics, Eq. (13) can be used to analyze and quantify TPD data without introducing significant error regardless of the degree of mixing within the TPD cell.

Estimated values of  $A_d$ , for first-order kinetics, are presented in Table 3. It is apparent that estimated values are always smaller than the true value of  $1.0 \times 10^{13} \text{ s}^{-1}$ , used in the simulation of the spectra. It is also apparent that very large errors can result from the existence of axial concentration gradients within the TPD cell. As the Peclet value approaches infinity (or the bed approaches PFR conditions) the estimated value of  $A_d$  is four to five orders of

magnitude less than the actual value. This is not the case when desorption follows second-order kinetics. Computed  $A_d$  values shown in Table 4 do not differ significantly from the true value.

These results seem to suggest that, for a given Peclet number and surface coverage, the gas phase concentration of the adsor-

TABLE 3

Estimated Preexponential Factors for Desorption,  $A_d$ , for First-Order Kinetics

$Pe_L$	$A_d \text{ (s}^{-1}\text{)}$		
	$S_0 = 10^{-4}$	$S_0 = 10^{-2}$	$S_0 = 10^0$
0	$1.0 \times 10^{13}$	$1.0 \times 10^{13}$	$1.0 \times 10^{13}$
0.8	$4.4 \times 10^{12}$	—	—
1.3	$3.1 \times 10^{12}$	$5.4 \times 10^{12}$	$8.6 \times 10^{12}$
1.9	$2.5 \times 10^{12}$	—	—
3.0	$1.1 \times 10^{12}$	$4.0 \times 10^{12}$	$5.6 \times 10^{12}$
6.7	$2.2 \times 10^{11}$	$6.2 \times 10^{11}$	$1.6 \times 10^{12}$
11.8	$2.5 \times 10^{10}$	—	—
$\infty$	$1.0 \times 10^8$	$5.7 \times 10^8$	$3.8 \times 10^9$

TABLE 4  
Estimated Preexponential Factors for Desorption,  $A_d$ , for Second-Order Kinetics

$Pe_L$	$A_d$ ( $s^{-1}$ )		
	$S_0 = 10^{-4}$	$S_0 = 10^{-2}$	$S_0 = 10^0$
0	$1.0 \times 10^{13}$	$1.0 \times 10^{13}$	$1.0 \times 10^{13}$
0.8	$9.9 \times 10^{12}$	—	—
1.3	$9.9 \times 10^{12}$	$9.8 \times 10^{12}$	$1.0 \times 10^{13}$
1.9	$9.8 \times 10^{12}$	—	—
3.0	$9.7 \times 10^{12}$	$9.8 \times 10^{12}$	$1.0 \times 10^{13}$
6.7	$9.0 \times 10^{12}$	$9.4 \times 10^{12}$	$1.0 \times 10^{13}$
11.8	$5.4 \times 10^{12}$	—	—
$\infty$	$3.0 \times 10^{12}$	$3.6 \times 10^{12}$	$4.5 \times 10^{12}$

bate is more uniform along the catalyst bed when desorption follows second-order kinetics. This is illustrated in Fig. 7 where

surface coverage at  $T_m$  is plotted as a function of dimensionless bed length for first- and second-order desorption kinetics. A value of  $10^0$  for the initial sticking coefficient was assumed. It is interesting to observe that in the plug flow case and for first-order kinetics, desorption moves in a front. The first part of the bed is initially depleted of adsorbate and, as temperature increases, desorption takes place from latter parts of the bed.

The perfectly mixed series of cells configuration was also used to model TPD experiments, following Eq. (7). The same trends concerning peak temperatures and computed values of  $\Delta H$  and  $A_d$  were observed. In the second-order desorption case, the error in the estimation of  $\Delta H$  was found to be less than 8% in all cases. In the first-order

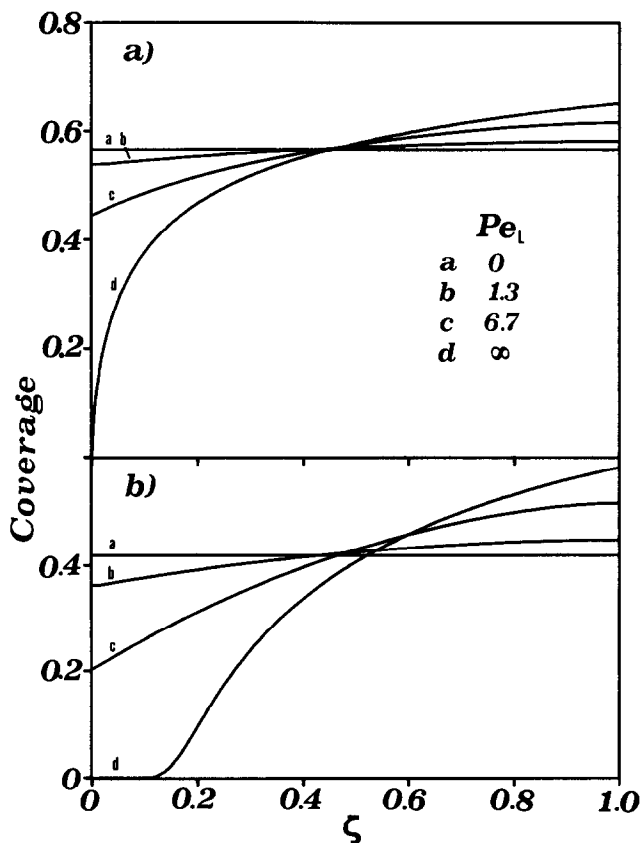


FIG. 7. Axial surface coverage profiles at  $T_m$  for different degrees of mixing within TPD cells. (a) Second order kinetics. (b) First-order kinetics.

desorption case the errors introduced are significantly higher.

#### CONCLUSIONS

The following conclusions can be drawn from the results of the present investigation:

1. As a result of axial concentration gradients within TPD cells, peak temperatures shift to lower values. For Peclet values less than 2, the shift in peak temperature is less than 5 K.

2. When desorption follows first-order kinetics, quantitative analysis of TPD spectra to obtain kinetic and thermodynamic parameters yields accurate results only under conditions of perfect mixing. The errors introduced are smaller than expected experimental uncertainties when the Peclet number is less than unity.

3. When desorption follows second-order kinetics, accurate estimates of heat of adsorption and preexponential factor of desorption can be made regardless of the degree of mixing within the TPD cell.

4. An assessment of the existence of axial gradients within a TPD bed can be obtained experimentally by variation of  $V_t$  and  $Q$  in such a way that their ratio is maintained

constant. Under such conditions, any shifts in peak temperature will be due only to different mixing conditions.

#### REFERENCES

1. Cvetanovic, R. J., and Amenomiya, Y., *Catal. Rev.* **6**, 21 (1972).
2. Falconer, J. L., and Schwarz, J. A., *Catal. Rev.-Sci. Eng.* **25**, 14 (1983).
3. Konvalinka, J. A., Scholten, J. J. F., and Rasser, J. C., *J. Catal.* **48**, 365 (1977).
4. Lee, P. I., and Schwarz, J. A., *J. Catal.* **73**, 272 (1982).
5. Rieck, J. S., and Bell, A. T., *J. Catal.* **85**, 143 (1984).
6. Criado, J. M., Malet, P., and Munuera, G., *Langmuir* **3**, 973 (1987).
7. Herz, K. R., Kiela, B. J., and Marin, P. S., *J. Catal.* **73**, 66 (1982).
8. Gorte, R. J., *J. Catal.* **75**, 164 (1982).
9. Demmin, R. A., and Gorte, R. J., *J. Catal.* **90**, 32 (1984).
10. Huang, Y.-J., Xue, J., and Schwarz, J. A., *J. Catal.* **109**, 396 (1988).
11. Jones, D. M., and Griffin, G. L., *J. Catal.* **80**, 40 (1983).
12. Tronconi, E., and Forzatti, P., *J. Catal.* **93**, 197 (1985).
13. Lemaitre, J. L., in "Characterization of Heterogeneous Catalysts" (F. Delannay, Ed.), p. 29. Dekker, New York, 1984.
14. Butt, J. B., "Reaction Kinetics and Reactor Design." Prentice-Hall, Englewood Cliffs, NJ, 1980.
15. Huang, Y.-J., and Schwarz, J. A., *J. Catal.* **99**, 249 (1986).